Mössbauer Spectroscopy

DOI: 10.1002/anie.201406710

Re-Appearance of Cooperativity in Ultra-Small Spin-Crossover [Fe(pz){Ni(CN)$_4$}] Nanoparticles**

Haonan Peng, Simon Tricard, Gautier Félix, Gábor Molnár, William Nicolazzi, Lionel Salmon, and Azzedine Bousseksou**

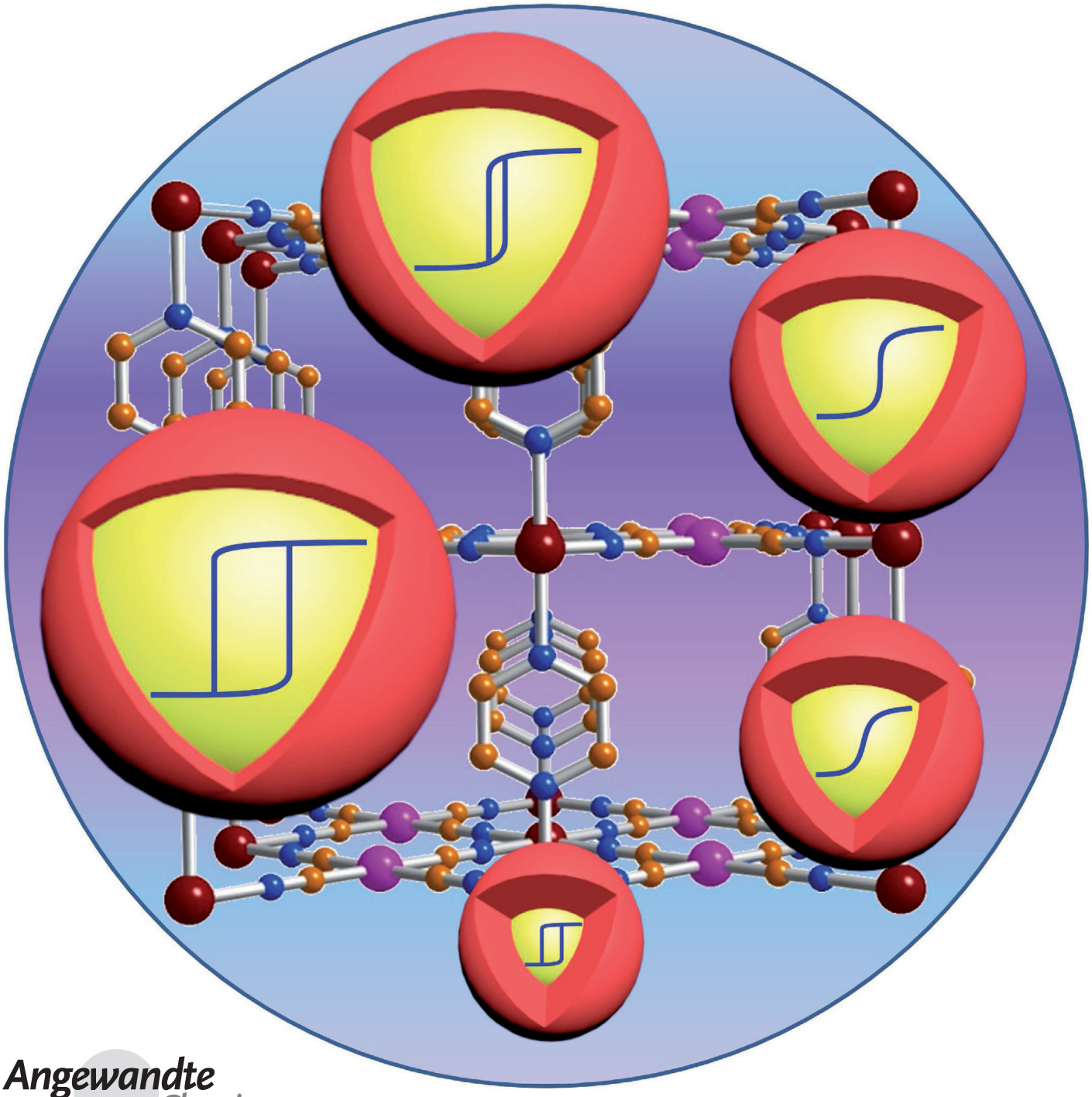

Abstract: *A reverse nanoemulsion technique was used for the elaboration of [Fe(pz){Ni(CN)$_4$}] nanoparticles. Low-temperature micellar exchange made it possible to elaborate ultra-small nanoparticles with sizes down to 2 nm. When decreasing the size of the particles from 110 to 12 nm the spin transition shifts to lower temperatures, becomes gradual, and the hysteresis shrinks. On the other hand, a re-opening of the hysteresis was observed for smaller (2 nm) particles. A detailed ^{57}Fe Mössbauer spectroscopy analysis was used to correlate this unusual phenomenon to the modification of the stiffness of the nanoparticles thanks to the determination of their Debye temperature.*

Recently, we have assisted a strong renewed interest in the field of molecular spin-crossover complexes as demonstrated by the emergence of nanosized spin-crossover materials through synthesis of coordination nanoparticles[1] and nanopatterned thin films.[2] Indeed, the synthesis of nanometer-sized spin-crossover (SCO) materials, their manipulation at reduced length scales, and the investigation of their size-dependent properties contribute to explore their possible practical applications in future nanophotonic, nanoelectronic, and spintronic devices. An important challenge in this context is to preserve the bistability and the cooperative spin-transition properties during the downsizing of the compound at the nanoscale. As it is well-known, the macroscopic behavior of bulk SCO materials is strongly influenced by electron–lattice coupling effects. In a first approximation, size reduction effects in spin-crossover materials are expected to occur primarily due to the reduction in the number of interacting metallic centers leading to the decrease of the cooperativity. Nevertheless, this picture is far too simplistic and many other parameters and material properties have to be considered in order to interpret the experimental observations obtained with SCO nanomaterials. In a very recent study,[3] we performed a ^{57}Fe Mössbauer spectroscopic study to follow the evolution of the elastic properties of coordination nanoparticles (particles without SCO) embedded in the same matrix as a function of their size. A sharp increase in the stiffness at very small particle sizes was observed. This study clearly shows that elastic properties of nanoparticles can change with the particle size. This implies many consequences in the case of spin-crossover materials. One hypothesis is that the surfaces are more rigid than the core of the particle. In a first time, a size decrease would lead to a decrease of cooperativity until a certain size. Then the influence of surfaces would become greater and there would be an increase of cooperativity. In order to better understand this phenomenon, the elastic properties of SCO particles with sizes between 3 and 30 nm have to be explored systematically and confronted with the theoretical models recently developed.[4] The objective of the present work was to synthesize and study the evolution of the spin-crossover properties of a complete series of [Fe(pz){Ni(CN)$_4$}] nanoparticles with different sizes, but with the same environment in order to demonstrate experimentally the influence of the surface and the particle stiffness on the cooperativity for nanoparticles with ultra-small sizes.

The reverse nanoemulsion technique was used for the elaboration of [Fe(pz){Ni(CN)$_4$}] nanoparticles with different sizes. In contrast with the previously reported synthesis methods[5,6] and with the objective to reach sizes down to 2–3 nm both the preparation of the starting nanoemulsion and the micellar exchange reaction were performed at low temperature. By modifying both the temperature and the concentration of the reactants nanoparticles with sizes from 2 to 107 nm could be obtained (see Table 1). It is interesting to note that a significant color change of the powder samples could be observed as a function of the particle size (see Figure 1). The darkening of the sample can be explained by the increasing residual low-spin (LS) fraction at room temperature when the size of the nanoparticles decreases. The composition of the samples was obtained thanks to combined thermogravimetric, elemental, and EDX (energy

Table 1: Sample preparation conditions, mean particle size (TEM), mean crystallite size (PXRD), and Debye temperature (^{57}Fe Mössbauer spectroscopy).

Sample	[Fe] [mol L^{-1}]	ω	T [K]	Particle size [nm]	Crystallite size [nm]	Debye temperature [K]
1	0.1	10	293	107 ± 14	29	171 ± 4
2[a]	0.1	10	293	71 ± 10	30	169 ± 5
3	0.15	10	293	12 ± 3	13	197 ± 9
4	0.15	10	243	3.1 ± 0.4	5.8	222 ± 4
5	0.2	10	258	2.0 ± 0.3	4.3	261 ± 6

[a] Fast mixture of the two nanoemulsion compared to **1** (see the Supporting Information).

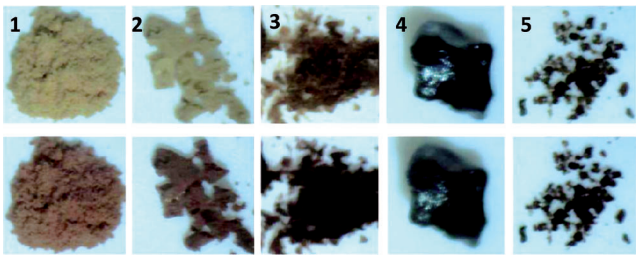

Figure 1. Color of the samples **1**–**5** at room temperature (top panel) and at liquid nitrogen temperature (bottom panel).

[*] H. Peng, Dr. S. Tricard, G. Félix, Dr. G. Molnár, Dr. W. Nicolazzi, Dr. L. Salmon, Dr. A. Bousseksou
Laboratoire de Chimie de Coordination, CNRS UPR-8241 and Université de Toulouse; UPS, INP
31077 Toulouse (France)
E-mail: lionel.salmon@lcc-toulouse.fr
azzedine.bousseksou@lcc-toulouse.fr

[**] The work was supported by the CROSS-NANOMAT project (ANR 2010-BLAN-7151) and the NANOHYBRID project (ANR-13-BS07-0020-01). H.P. thanks the China Scholarship Council for a PhD grant and ST the European Commission for a postdoctoral grant (PCIG11-GA-2012-317692).

Supporting information for this article is available on the WWW under http://dx.doi.org/10.1002/anie.201406710.

dispersive X-ray) analyses (see the experimental section in the Supporting Information):
$[Fe(Pyrazine)Ni(CN)_4]\cdot 0.7\,H_2O$ (**1**),
$[Fe(Pyrazine)Ni(CN)_4]\cdot 0.8\,H_2O\cdot 0.02\,S$ (**2**),
$[Fe(Pyrazine)_{0.6}Ni(CN)_4]\cdot 0.6\,H_2O\cdot 0.2\,S$ (**3**),
$[Fe(Pyrazine)_{0.3}Ni(CN)_4]\cdot 1\,H_2O\cdot 0.08\,S$ (**4**),
$[Fe(Pyrazine)_{0.2}Ni(CN)_4]\cdot 1\,H_2O\cdot 0.13\,S$ (**5**)
and S is the NaAOT (sodium bis(2-ethylexyl sulfosuccinate) surfactant.

Transmission electron microscopy (TEM) and high-resolution transmission electron microscopy (HRTEM) were used to determine the size of the nanoparticles. Figure 2 shows a selected TEM image for each sample (complementary images are reported in the Supporting Information). As reported in Table 1, the control of the experimental conditions permits us to obtain a sample series with nanoparticle sizes ranging from 2.0 to 107 nm (this size corresponding to the in-plane width). As already reported for numerous nanoparticle syntheses and validated for the elaboration of $[Fe(pz)\{Pt(CN)_4\}]$ derivative nanoparticles, increasing the reactants concentration, while maintaining constant the polar phase/surfactant molar ratio (ω), leads to the decrease of the mean size of the nanoparticles. Nevertheless, while playing with the concentration, it was not possible to decrease the nanoparticle size below approximately 12 nm because of the insolubility of the starting materials. Comparison of the TEM images for samples **1** and **2** shows that the addition speed of the emulsions plays also a key role on the nanoparticle size. Eventually, reducing the reaction temperature to 243 K permitted us to reach nanoparticle sizes lower than 4 nm. We tried to reduce even further the reaction temperature, but these experiments resulted repetitively in the immediate destabilization of the nanoemulsions.

HRTEM associated with energy dispersive X-ray spectrometry was used to try to better characterize the morphology and the composition of the nanoparticles. Figure 2 shows HRTEM images of sample **4** (see also the Supporting Information for HRTEM images for the other samples and EDX measurements) where one can distinguish the ultrasmall particles (mean size about 3 nm). Moreover, energy dispersive X-ray spectrometry (EDX) was also employed in order to determine the composition of the particles. Whatever the area considered, from 1 nm^2 (single particle) to 0.2 μm^2 (several dozens of particles), the quantitative EDX analyses showed equivalent percentage of iron and nickel atoms confirming in agreement with the following PXRD and

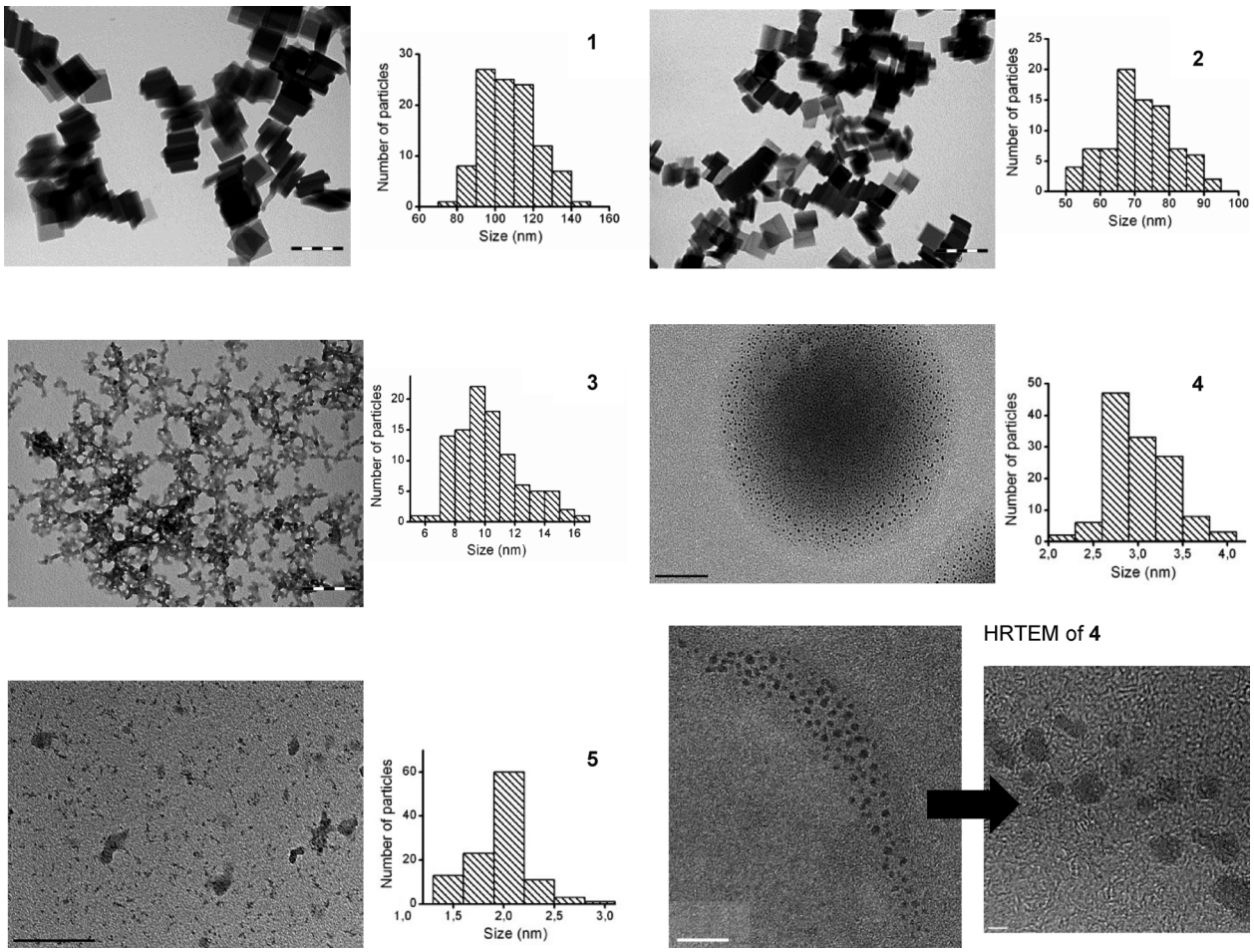

Figure 2. TEM images and associated size distribution histograms of samples **1**–**5** and HRTEM images of sample **4**. The scale bars in the TEM images are 200 nm for samples **1** and **2**, 300 nm for sample **3**, 100 nm for sample **4**, and 100 nm for sample **5**. The scale bar in the section of the TEM image of sample **4** is 10 nm and the scale bar in the HRTEM image of sample **4** is 2 nm.

Raman data, the presence of the Fe(pyrazine)$_x$[Ni(CN)$_4$] complex.

Figure S12 shows the powder X-ray diffraction (PXRD) patterns of the differently sized nanoparticle samples. The pattern observed for the bulk sample[7] corresponds to those measured for each nanoparticle sample, but a significant increase of the peak widths is observed when the size of the nanoparticles is decreasing. X-ray diffraction allows also for the estimation of the crystallite size using the Scherrer equation (see the Supporting Information for details). The average crystallite size for each sample are gathered in Table 1 and compared with the nanoparticle sizes obtained by transmission electronic microscopy. For the smaller particles, the sizes of the crystallites are similar or slightly larger than those found with the TEM; this effect could be explained by the uncertainty of the PXRD method for these nanoparticle sizes. For sample **3**, the size of the crystallites is in agreement with the mean nanoparticle size indicating that the nanoparticles are composed by only one domain. Eventually, larger nanoparticles and also the bulk sample are composed of several domains of about 30 nm.

With the aim to determine more precisely the fraction of iron centers involved in the spin transition, and suitably calibrate the magnetic measurements, we have recorded the ^{57}Fe Mössbauer spectra for the different samples at different temperatures (Figure S18–S22). Whatever the sample, at 310 K the Mössbauer spectrum consists of two doublets, both with an isomeric shift δ close to 1 mm s^{-1} and large quadrupole spittings ($\Delta E_Q = 1.2$ and 2 mm s^{-1}) typical of a high-spin (HS) iron(II) ($S = 2$). In addition, a third LS doublet with isomeric shift δ close to 0.4 mm s^{-1} appears for smaller nanoparticles. The 10% fraction associated with the large quadrupole splitting HS species in each sample can be explained by the presence of defects in the coordination network. The increasing residual LS fraction while the size of the nanoparticles decrease, 8% for 12 nm particles, 16% for 3 nm particles, and 56% for 2 nm particles might be related to the increase of the quantity of iron atoms localized at the surface of the nanoparticles. When the samples are cooled down, the area of the HS doublet with the smallest quadrupole-splitting decreases and, conversely, the area of the LS doublet increases; whereas the area of the HS doublet with the large quadrupole-splitting remains constant. The variable temperature Mössbauer spectrum (from 310 to 80 K) for samples **1**–**5** reveals that while decreasing the size of the nanoparticles, the fraction of the SCO-active species decreases from 77% for sample **1** to 7% for sample **5** (77% for sample **2**, 58% for sample **3,** and 23% for sample **4**).

The thermal variation of the high-spin fraction n_{HS} in the samples (Figure 3) was deduced from the magnetic susceptibility data thanks to the determination of the residual HS and LS fractions in the low- and high-temperature regions by Mössbauer spectroscopy and the sample composition by TGA and elemental analysis. Although a small shift of the transition curves to higher temperatures is observed after the isothermal holding of samples,[7] all experiments have been realized on dehydrated samples. As expected, the large particles present physical properties similar to the bulk sample with a spin transition close to room temperature

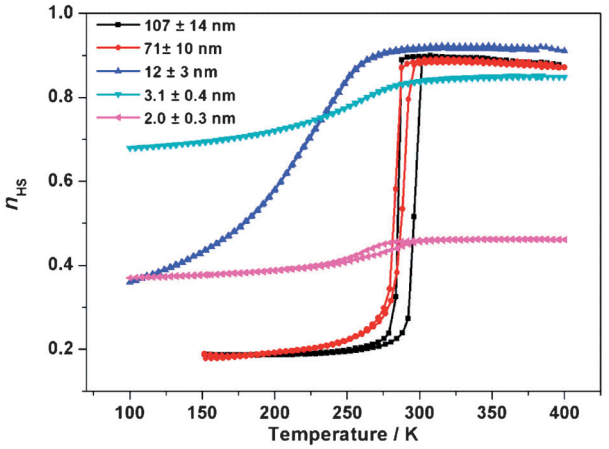

Figure 3. Calibrated $n_{HS} = f(T)$ curves for samples **1**–**5** obtained from magnetic and Mössbauer measurements.

with a hysteresis loop.[8] The decrease of the size to 12 nm leads, as already reported,[5] to a more gradual transition without hysteresis and with a shift to lower temperature. The modification of the spin-crossover behavior is also accompanied by an increase of the residual HS fraction at low temperature. Nanoparticles with sizes of about 3 nm revealed an even higher residual HS fraction and also some residual LS fraction together with an apparent re-increase of the transition temperature. These effects were more clearly demonstrated in the case of the smallest 2 nm particles exhibiting important "inactive" HS and LS fractions, a higher transition temperature and even the re-opening of the hysteresis loop. This latter phenomenon was predicted in our recent article theoretically,[3] but it is the first time that an experimental demonstration could be achieved.

Using the Debye model one can determine the so-called "Mössbauer Debye temperature", θ_D from the temperature dependence of the full area (A) of the Mössbauer spectrum.[9,10] A higher value of θ_D signifies that the crystal lattice is stiffer. A least-squares fit of ln[A] versus T allowed us to determine the values of θ_D (see the Supporting Information). Figure 4 represents the variation of θ_D as a function of the

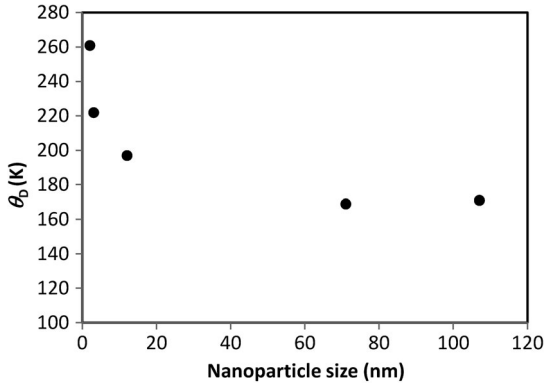

Figure 4. Variation of the Debye temperature as a function of the size of the particles. (The statistical error is comparable with the size of the symbols.)

nanoparticle size. For the larger nanoparticles (107 and 71 nm) the same θ_D value of about 170 ± 4 K was measured. The decrease of the particle size to 12 nm leads to a significant increase of θ_D to 197 ± 9 K. Finally, samples with the smallest nanoparticle sizes revealed a very important increase of θ_D with 222 ± 4 K for sample **4** and 261 ± 6 K for sample **5**. It is worth noting that the θ_D value measured for the small nanoparticles is underestimated taking into account the important HS residual fraction in the considered low-temperature range. Indeed, as it is well-known when going from the HS to the LS state the spin-crossover phenomenon is accompanied by a lattice contraction which tends to increase the θ_D value. These measurements undeniably put in evidence an increase of the θ_D value when decreasing the nanoparticle size below approximately 15–20 nm. This increase of the θ_D value reveals thus an increase of the stiffness of the nanoparticles. In view of these experimental results, we suggest that the re-increase of the cooperativity observed for the smallest nanoparticles is closely related to the increase of the stiffness of particles. In order to explain these behaviors we can suggest that two independent mechanisms have to be considered when the nanoparticle size is decreasing. On one hand, as explained in Ref. [3] the increasing surface-to-volume ratio leads to the downshift of the spin-transition temperature and the loss of hysteresis. On the other hand the increase of the stiffness of the particles in ultra-small particles leads to an opposite effect. (See the Supporting Information for details of the theoretical model.) Additionally, despite the fact that the X-ray powder pattern is similar for all the samples, the presence of a single domain (only one crystallite per particle) and/or a possible modification of the shape of the particles[4a] could also play an important role on the SCO properties. Indeed, for samples **4** and **5**, TEM and HRTEM measurements seem to show nanoparticles with rather a spherical shape in contrast to the cubic shape encountered for larger nanoparticles. Finally, even if the matrix is different, the unexpectedly strong cooperativity reported previously for the 3 nm Fe(pyrazine)[$Ni(CN)_4$] nanoparticles embedded in chitosan supports also the present results.[7]

In conclusion, nanoreactors built using reverse nanoemulsion were used for the synthesis of a series of [Fe(pz){$Ni(CN)_4$}] nanoparticles with sizes ranging from 2 to 107 nm and with the same NaAOT matrix. For the first time it was possible to obtain a series of ultra-small nanoparticles smaller than 15 nm. Composition and size of the particles were probed with TEM and HRTEM investigations associated with EDX analyses. The size diminution was also evidenced by X-ray powder diffraction analyses through the determination of the crystallite size with the Scherrer equation. Raman (see the Supporting Information) and Mössbauer spectroscopy and magnetic measurements were combined to determine the spin-crossover behavior with accuracy for the different samples. The results obtained for the larger [Fe(pz){$Ni(CN)_4$}] nanoparticles (107, 71 and 12 nm) namely the loss of the cooperativity, the shift of the transition to lower temperatures, and the increase of the residual HS fraction at low temperature for a decreasing size, corroborate previous reports obtained for the analogous [Fe(pz){$Pt(CN)_4$}] nanoparticles. On the other hand, the properties of the ultra-small particles (2 and 3 nm) revealed a re-increase of the cooperativity and of the transition temperature with even the re-opening of a hysteresis loop for the smallest nanoparticles. In order to find an origin to this unexpected behavior for such small SCO nanoparticles, we carried out a detailed Mössbauer study to determine the stiffness of the different nanoparticles by measuring their Debye temperature and we revealed a significant increase of θ_D for the smallest nanoparticles. Thus, the unusual SCO properties observed at low size can be explained thanks to the consideration of the size-dependent elastic properties of the particles which is related to the strain induced by the surface.

Received: July 1, 2014
Revised: July 22, 2014
Published online: August 26, 2014

Keywords: Debye temperature · Mössbauer spectroscopy · nanoparticles · spin crossover · transition metals

[1] a) A. Bousseksou, G. Molnár, L. Salmon, W. Nicolazzi, *Chem. Soc. Rev.* **2011**, *40*, 3313 – 3335, and references therein; b) H. J. Shepherd, G. Molnár, W. Nicolazzi, L. Salmon, A. Bousseksou, *Eur. J. Inorg. Chem.* **2013**, 653 – 661, and references therein; c) M. Mikolasek, G. Félix, W. Nicolazzi, G. Molnár, L. Salmon, A. Bousseksou, *New J. Chem.* **2014**, *38*, 1834 – 1839.

[2] M. Cavallini, *Phys. Chem. Chem. Phys.* **2012**, *14*, 11867 – 11876, and references therein.

[3] G. Félix, W. Nicolazzi, L. Salmon, G. Molnár, M. Perrier, G. Maurin, J. Larionova, J. Long, Y. Guari, A. Bousseksou, *Phys. Rev. Lett.* **2013**, *110*, 235701.

[4] a) G. Félix, W. Nicolazzi, M. Mikolasek, G. Molnár, A. Bousseksou, *Phys. Chem. Chem. Phys.* **2014**, *16*, 7358 – 7367; b) T. Kawamoto, S. Abe, *Chem. Commun.* **2005**, *31*, 3933 – 3935; c) A. Muraoka, K. Boukheddaden, J. Linarès, F. Varret, *Phys. Rev. B* **2011**, *84*, 054119; d) L. Stoleriu, P. Chakraborty, A. Hauser, A. Stancu, C. Enachescu, *Phys. Rev. B* **2011**, *84*, 134102; e) H. Oubouchou, A. Slimani, K. Boukheddaden, *Phys. Rev. B* **2013**, *87*, 104.

[5] F. Volatron, L. Catala, E. Rivière, A. Gloter, O. Stéphan, T. Mallah, *Inorg. Chem.* **2008**, *47*, 6584 – 6586.

[6] I. Boldog, A. Gaspar, V. Martinez, P. Pardo-Ibanez, V. Ksenofontov, A. Bhattacharjee, P. Gütlich, J. Real, *Angew. Chem.* **2008**, *120*, 6533 – 6537; *Angew. Chem. Int. Ed.* **2008**, *47*, 6433 – 6437.

[7] J. Larionova, L. Salmon, Y. Guari, A. Tokarev, K. Molvinger, G. Molnár, A. Bousseksou, *Angew. Chem.* **2008**, *120*, 8360 – 8364; *Angew. Chem. Int. Ed.* **2008**, *47*, 8236 – 8240.

[8] V. Niel, J. M. Martinez-Agudo, M. C. Muñoz, A. B. Gaspar, J. A. Real, *Inorg. Chem.* **2001**, *40*, 3838 – 3839.

[9] N. N. Greenwood, T. C. Gibb, *Mössbauer spectroscopy*, Chapman and Hall Ltd. London, **1971**.

[10] K. Boukheddaden, F. Varret, *Hyperfine Interact.* **1992**, *72*, 349 – 356.

